Preprint / *Nitric Oxide* / 2019 https://doi.org/10.1016/j.niox.2019.01.014

Acceleration of the Autoxidation of Nitric Oxide by Proteins

Matías N. Möller and Ana Denicola

Laboratorio de Fisicoquímica Biológica, Instituto de Química Biológica, Facultad de Ciencias, and Center for Free Radical and Biomedical Research, Universidad de la República, Igua 4225, CP11400, Montevideo, Uruguay
Corresponding authors: mmoller@fcien.edu.uy and denicola@fcien.edu.uy

Abstract

Lipoproteins and lipid membranes accelerate •NO autoxidation by increasing local concentration of •NO and O_2. Although the idea that proteins could also accelerate this reaction was presented some time ago, it was largely criticized and dismissed. Herein the effect of proteins on •NO autoxidation rates was studied following •NO disappearance with a selective electrode. It was found that human serum albumin (HSA) accelerated •NO autoxidation by a factor of 9 per g/mL of protein, much less than previously suggested. The acceleration by HSA was sensitive to pH and significantly decreased at pH lower than 4.5 coincident with the acid structure transition of HSA to a partially unfolded and rigid conformation. Other proteins with different surface hydrophobicity also accelerated •NO autoxidation and it was found to depend mostly on the protein size and dynamics. Mathematical simulations were performed to assess the physiological importance of this acceleration. It was calculated that in plasma the autoxidation of •NO is accelerated 1.38 times by HSA relative to water alone, but this becomes of little relevance when whole blood is simulated because of the rapid rate of •NO consumption by red blood cells.

Introduction

Nitric oxide is an important signaling molecule produced biologically by the enzymes nitric oxide synthases (NOS) that are expressed differentially in different tissues. There are two constitutive NOS isoforms (type I neuronal NOS, and type III endothelial NOS) and one inducible NOS (iNOS, type II). In the vascular system predominates the endothelial NOS (eNOS) located in endothelial cells that produces •NO as a response to different stimuli and induces vasorelaxation [1]. The biological effects of •NO depend on its reactivity towards biological targets. Despite being a free radical, •NO is not very reactive and preferentially reacts with other radical species such as superoxide anion, lipid peroxyl radicals and metals in metalloproteins [2]. The reaction with ferrous heme in soluble guanylate cyclase is one of the most important signal transduction mechanisms of •NO, leading to an increase in the production of cGMP that activates cGMP-kinases and membrane ion channels, decreases intracellular calcium levels and allows smooth muscle to relax [3]. Another important reaction is that with superoxide to yield the potent oxidant peroxynitrite that not only oxidizes cysteine and methionine residues but is also capable of nitrating tyrosines, a footprint of this biological oxidant [4].

Nitric oxide also reacts with O_2, in a complex reaction yielding oxidizing and nitrosating products ($^{\bullet}NO_2$ and N_2O_3) that in water are hydrolyzed to nitrite [5, 6]:

$$2\ {}^{\bullet}NO + O_2 \rightarrow 2\ {}^{\bullet}NO_2 \qquad \text{(Eq. 1)}$$

$$^{\bullet}NO_2 + {}^{\bullet}NO \rightleftharpoons N_2O_3 \qquad \text{(Eq. 2)}$$

$$N_2O_3 + H_2O \rightarrow 2\ NO_2^- + 2\ H^+ \qquad \text{(Eq. 3)}$$

The autoxidation of •NO is kinetically an overall third-order reaction, which is second-order to •NO and first-order to O_2:

$$dNO / dt = 4k_3[{}^{\bullet}NO]^2[O_2] \qquad \text{(Eq. 4)}$$

In water, the third-order rate constant k_3 has values that range between 1.5 and 3.0 × 10^6 $M^{-2}s^{-1}$ [5-8]. Given the low concentrations of •NO attained *in vivo*, and the dependence of the rate on the square of the concentration of •NO, this reaction is considered too slow to be biologically relevant. However, it was later shown that lipid membranes and lipoproteins, which have a well-defined hydrophobic interior, accelerate this reaction by a factor of 30 to 300 relative to the

rate in water [6, 9], and it was shown to occur because of the favored partitioning of •NO and O_2 in the hydrophobic regions [6]. The solubility of these molecules in lipid membranes has been recently related to the available free volume formed as a result of molecular mismatch and thermal motions [10, 11]. The autoxidation of •NO was also observed to be accelerated by mitochondria and submitochondrial particles [12].

Some years ago it was proposed that the hydrophobic core of serum albumin could accelerate the autoxidation of •NO four orders of magnitude relative to the aqueous phase [13, 14]. This report was received with skepticism and the predictions on the increase of thiol nitrosation in the presence of albumin were later refuted [15]. Proteins are not as "spongy" as lipid membranes and show average densities similar to organic crystals [16]. Nevertheless, proteins are not perfectly packed and hydrophobic cavities are present in their structure [16] that have been shown to accommodate hydrophobic molecules [17, 18]. Furthermore, proteins undergo structural fluctuations in the nanosecond range and therefore are dynamic rather than rigid structures [19]. This was evidenced by O_2 quenching of tryptophan fluorescence in a wide range of proteins, including proteins with internal tryptophans that are not accessible to the solvent [19]. The diffusion coefficients of O_2 in the protein matrix are only 20% of that in water, indicating that despite the rigid picture given by crystal structures, proteins are very dynamic [19]. Considering the presence of hydrophobic cavities and the dynamics of proteins we thought that proteins could indeed accelerate •NO autoxidation, albeit at lower rates than reported, and this issue merited further study.

In this work we determined the rate of •NO reaction with O_2 using an •NO-selective electrode, which allows direct observation of any acceleration in the •NO disappearance rates produced by proteins. We focused on human serum albumin (HSA), which is the most abundant protein in human plasma, but other proteins such as ovalbumin (OVA), lysozyme (LYS) and trypsin (TRY) were also assayed for comparison. The observed acceleration factors were correlated with several molecular properties, including the volume of the cavities within the protein structure. Finally, a mathematical model was constructed including the most important reactions of •NO that could reproduce the experimental results, and allowed us to extrapolate our findings to a biological scenario like the blood vessel, to understand the fate of the different species and the relative importance of accelerated •NO autoxidation by HSA.

Materials and Methods

Materials. Prolinonoate was from Alexis Biochemicals (San Diego, California). All other reagents were from Sigma (St Louis, MO). Most experiments were done in 100 mM phosphate buffer with 100 µM DTPA at pH 7.4 at 25°C. Solutions of different pH were prepared by adding HCl to this buffer and then checking the final pH. The solution at pH 3.3 was done using 100 mM citric acid with 100 µM DTPA. Human serum albumin (HSA) was delipidated as described [20] and then equilibrated in buffer by gel filtration. Other proteins were prepared directly in buffer by weight, re-equilibrated in buffer by gel filtration and the final concentration was determined by absorbance at 280 nm. This was done to ensure exactly the same buffer composition in the different experiments. This is particularly important since the solubility of both •NO and O_2 is sensitive to the concentration of dissolved salts and would affect the association to proteins. In •NO autoxidation assays, the buffer used as reference was the same buffer used to dissolve the proteins.

•NO autoxidation assays. The disappearance of •NO by autoxidation was followed using an •NO-selective electrode coupled to an Apollo 4000 analyzer (WPI Inc, Sarasota, FL). The system has a custom-made reaction glass chamber of 1300 µL and a cap that allows insertion of the •NO probe and a capillary to inject •NO into the chamber using a gastight Hamilton Syringe. The absence of headspace and the capillary ensured that gas exchange (loss of •NO) to the environment was minimal. The chamber also includes a water jacket connected to a thermostatted circulating water bath at 25 ºC. The electrode was calibrated as described [6, 21] and prolinonoate was prepared as before and quantitated using the calibrated electrode [6]. The •NO autoxidation assay consisted in adding ~8 µM •NO from a concentrated solution of prolinonoate to the closed chamber containing air-equilibrated buffer (or protein solution) and registering •NO decay in time. The acceleration factor A_C (Eq. 6) was determined for each protein using four different concentrations of

protein by duplicate, in at least three repeated experiments.

Determination of cavity volume in proteins. The molecular volume and surface area of proteins was determined using the "volume calculation" tool available in the 3V web server [22], using a probe of radius 1.5 Å, equivalent to a molecule of water. The structures were downloaded from the Protein Data Bank (RCSB PDB) and were PDB ID: 1E78 for HSA [23], PDB ID: 1S81 for trypsin [24], PDB ID: 1OVA for ovalbumin [25] and PDB ID: 1LYS for lysozyme [26]. The "solvent extraction" tool was used to determine the total volume and surface of the cavities in the structure of the different proteins, as well as to extract the 3D representation of the cavities. The outer probe and the inner probe radii were set to 1.5 and 0.5 Å, respectively, in order to discard clefts and only consider cavities within the protein that are not readily accessible to the solvent. The visualization was done using Chimera [27].

Mathematical simulations. The complete system was modeled in Copasi, that is freely available [28], using irreversible or reversible mass action with the rate constants described in Table II. The initial concentration of most components was zero, except prolinonoate that was set to 4 µM, O_2 to 220 µM and HSA to 660 µM. The only included thiyl radical reaction was with •NO, because HSA is sterically hindered to make disulfides that can lead to superoxide [15]. The complete Copasi file is provided as supplementary material.

Results

Acceleration of •NO autoxidation by HSA. The autoxidation of •NO was studied after injecting 8 µM •NO from a prolinonoate stock solution to either 100 mM phosphate, 100 µM DTPA, pH 7.4 buffer or to defatted HSA solution in buffer. Prolinonoate is a rapid-release •NO donor that was used to ensure a correct mixing and avoid the high local concentration of a pure •NO bolus addition that could lead to experimental artifacts. The reaction was followed using an •NO -selective electrode as before [6].

Given that the •NO autoxidation rate is second-order relative to •NO, the integration of the rate equation is Eq. 5,

$$\frac{1}{[NO]} = k_{obs}t + \frac{1}{[NO]_0} \qquad \text{(Eq. 5)}$$

Therefore, there is a linear dependence between 1/[•NO] and time, and the slope is k_{obs} (Fig. 1B, black trace). This k_{obs} stands for $4k_3[O_2]$, where O_2 is in excess (220 µM), and k_3 is the third-order rate constant for •NO autoxidation. For these experiments k_3 in buffer was 2.8×10^6 $M^{-2}s^{-1}$, in agreement with previous results [5-8]. When the experiment was done

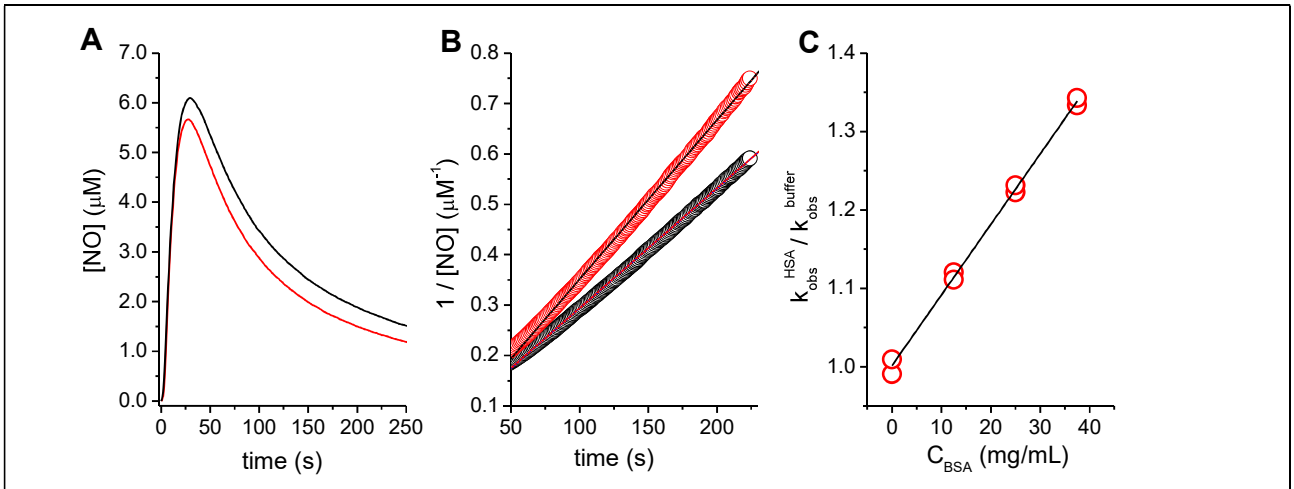

Figure 1. Acceleration of •NO autoxidation by HSA. A) •NO autoxidation was studied by following •NO disappearance using an NO-selective electrode in a sealed chamber with no headspace. 8 µM •NO was added from prolinonoate at time 0 in buffer alone (black) or in the presence of 37.5 mg/mL HSA (red). **B)** Linearization of the second-order reaction on •NO. The slopes are the pseudo-second-order rate constants of autoxidation (k_{obs}). The higher rate of autoxidation by HSA is observed as a greater slope. **C)** The increase in rate was proportional to protein concentration. The slope of this plot gives the acceleration factor $A_C = 9$ $(g/mL)^{-1}$ for HSA at 25°C and pH 7.4.

 https://doi.org/10.1016/j.niox.2019.01.014

in the presence of HSA, an increase in •NO autoxidation rate was observed (Fig. 1A, red trace) that is more evident in the linear fitting to the second-order reaction (Fig. 1B, red trace). The increase in •NO autoxidation rate was directly proportional to the concentration of HSA (Fig. 1C).

To evaluate the effect of HSA on the rate of •NO autoxidation, we introduced the term "A_C", that stands for *acceleration* and indicates how much the reaction rate is affected by HSA [6]:

$$k_{obs}^{HSA} / k_{obs}^{buffer} = 1 + A_C \times C_{HSA} \qquad \text{(Eq. 6)}$$

Therefore, we can determine the factor A_C from the slope of a secondary plot such as in Figure 1C, and A_C = 9 $(g/mL)^{-1}$ was obtained for HSA at 25°C and pH 7.4.

Is it a core or a surface effect? The acid transition of HSA. HSA undergoes an important conformational change below pH 4.3, leading to an "open" form which has a higher surface area and a lower volume and compressibility [29-31]. Therefore, the importance of protein surface *vs* core effects in •NO acceleration could be assessed by following the ability of HSA to accelerate the autoxidation of •NO at different pHs. It was observed that the acceleration factor A_C slightly increased at pH 6.5 and then decreased at lower pH, with no acceleration below pH 3.5. A pK_a of 4.5 was calculated for this process, that matches the pK_a for the acid transition of HSA. The basic transition occurs with pK_a = 8 [29]. Although it was not experimentally studied (because release of •NO from prolinonoate slows down at higher pH), it was introduced into the mathematical model and explains why acceleration is maximal at pH 6.5 (Figure 2).These results suggest that the acceleration of •NO autoxidation in the presence of HSA does not occur by adsorption to hydrophobic patches on the surface of the protein, because this surface hydrophobicity increase with the acid transition of HSA [29-31]. On the other hand, the compressibility and volume of the protein decrease when decreasing pH, in a similar manner to the observed results [30] and suggest an important role of the hydrophobic cavities and protein dynamics in accelerating •NO autoxidation.

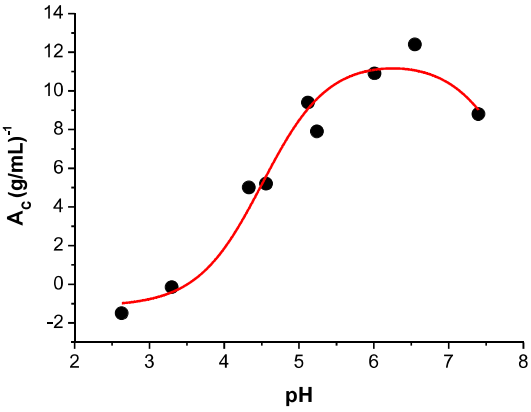

Figure 2. Acceleration of •NO autoxidation by HSA at different pH. The acceleration of •NO autoxidation by HSA change with pH and the transitions were determined by fitting to a model with two pK_a (trace). The decrease at lower pH with a pK_a = 4.5 matched the acid transition of HSA that leads to conformational changes including an increase in surface area and decrease in volume and compressibility.

Is it a core or surface effect? Comparison with other proteins. HSA has many hydrophobic surface patches that serve as binding pockets to many ligands [29]. However, the results on •NO autoxidation acceleration by HSA at different pHs suggested that it was not a surface effect. To further confirm this, we selected proteins that have a more polar surface than HSA, such as trypsin, lysozyme and ovalbumin, to determine whether they would be capable of accelerating •NO autoxidation. It was found that these proteins also accelerated •NO autoxidation but to different degrees (Fig. 3A and Table I). Whereas the acceleration by ovalbumin was similar to that of HSA, the acceleration by trypsin was nearly null.

We sought for correlations between the A_C coefficients and different molecular properties like volume, density and molecular weight (Table I). A very good correlation was found between A_C and protein adiabatic compressibility (Figure 3B, R^2 = 0.952). This compressibility is related to fluctuations in atom packing in the protein and is an indicator of protein flexibility [32-34], underscoring the

 https://doi.org/10.1016/j.niox.2019.01.014

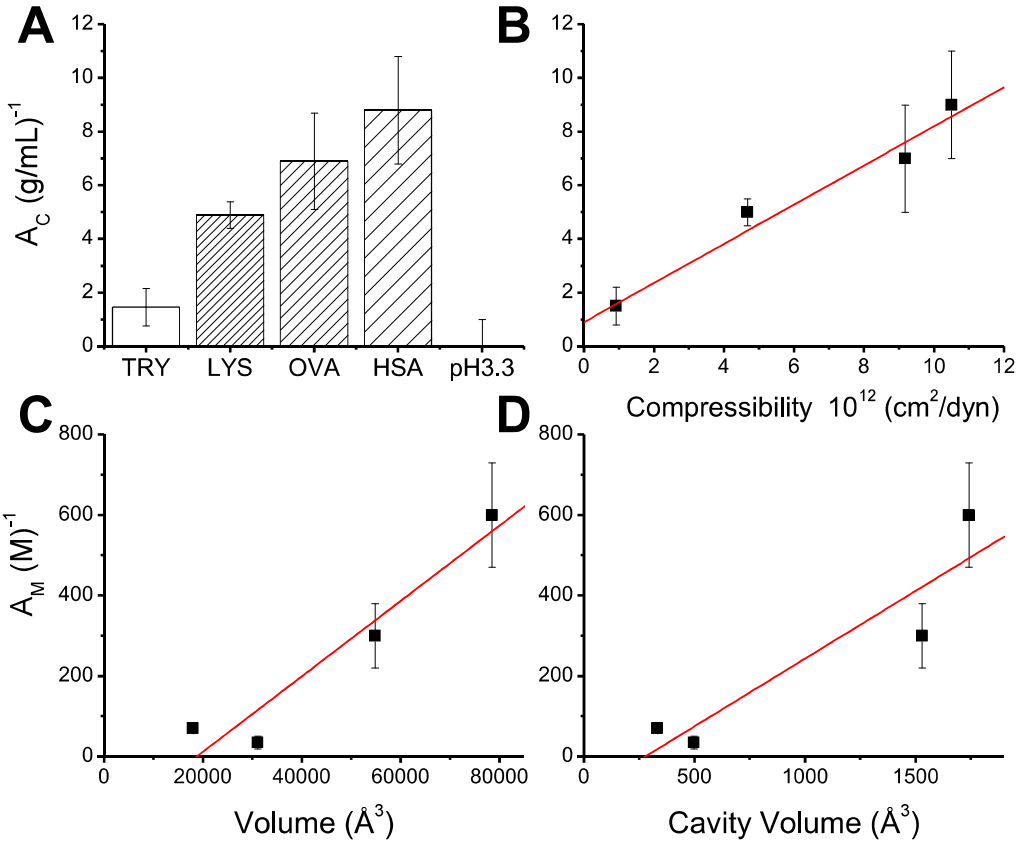

Figure 3. A) Acceleration of ˙NO autoxidation by different proteins: trypsin (TRY), lysozyme (LYS), ovalbumin (OVA) and human seroalbumin (HSA). It can be observed that proteins that have a more hydrophilic surface than HSA are also able to accelerate the autoxidation of ˙NO. **B)** A good correlation between Ac and protein compressibility was found (R^2 = 0.952), indicating that protein dynamics is an important factor regulating acceleration. **C)** The correlation between A_M (Ac x MW) and molecular volume was not so good (R^2 = 0.88) and suggests a minimum volume is required to allow acceleration of ˙NO autoxidation. **D)** The correlation between A_M and cavity volume was poor (R^2 = 0.77), suggesting that this factor affects acceleration in a nonlinear way.

importance of protein dynamics in accelerating ˙NO autoxidation.

To correctly correlate with molecular properties, the acceleration coefficient per Molar was used ($A_M = A_C \times MW$). In this case there were generally good correlations with most properties considered. Analysis of these correlations suggest that a minimum protein volume is necessary in order to accelerate ˙NO autoxidation (Figure 3C). Correlation with molecular volume was actually stronger than with cavity volume (R^2 = 0.88 vs 0.77, Figures 3C and 3D), suggesting that protein cavities affect acceleration in a nonlinear way.

Therefore, the acceleration of ˙NO autoxidation seems to depend mainly on two factors, the size and the dynamics of the protein, and not the hydrophobic surface of the protein.

Physiological importance of ˙NO autoxidation acceleration by HSA. To understand the significance of this acceleration of ˙NO autoxidation in blood, we performed mathematical simulations of the reactions involved in ˙NO autoxidation. The reactions used for the simulation represent a minimal model and are listed in Table II.

 https://doi.org/10.1016/j.niox.2019.01.014

Table I. Acceleration factors of ˙NO autoxidation and physical properties of the proteins

	MW (kDa)	A_C * $(g/mL)^{-1}$	A_M $(M)^{-1}$	Volume (Å^3)	Cavity volume (Å^3)	$\bar{\nu}$ (mL/g)	Compressibility 10^{12} (cm^2/dyn)
HSA	66.5	9 ± 2	600 ± 130	78545	1742	0.733	10.5
HSA/pH 3.3	66.5	0 ± 1	0				
OVA	42.8	7 ± 2	300 ± 80	54851	1530	0.746	9.18
TRY	23.5	1.5 ± 0.7	35 ± 16	31048	496	0.719	0.92
LYS	14.3	4.9 ± 0.5	70 ± 7	17951	331	0.712	4.67

* The reported A_C is the average value of three independent experiments plus minus the standard deviation.

The model represented the experimental results very well, after adjusting some parameters (R^2 = 0.9995, Figure 4A). In particular, the rate of injection of prolinonoate (Reaction 1 in Table II), the rate of ˙NO release from prolinonoate (Reaction 2 in Table II), and the exact amount of prolinonoate used (4.35 µM) were obtained by fitting the model to the experimental results of ˙NO disappearance in buffer. The rate of ˙NO autoxidation obtained by fitting the model was practically the same to the one obtained in Figure 1 by linearization (2.7 and 2.8 × 10^6 $M^{-2}s^{-1}$, respectively). These parameters obtained by model optimization were then included to simulate the acceleration by HSA, using the experimentally determined acceleration at 37.5 mg/mL HSA (Figure 1C), and a very good fit was obtained (R^2 = 0.9983, Figure 4A).

Next, to simulate the acceleration of ˙NO autoxidation in plasma by HSA, we considered the concentration of HSA in plasma (42 mg/L, [29]) and the acceleration factor A_C determined herein (Table I). An overall acceleration of 1.38 times by HSA in whole plasma was calculated. The addition to the model of reactions between $^{\cdot}NO_2$, N_2O_3 and HSA (reactions 6-8 in Table II) had no effect on the ˙NO disappearance rate, as expected for a process limited by ˙NO autoxidation. In the absence of HSA, transient concentrations of $^{\cdot}NO_2$ and N_2O_3 reached picoMolar levels, and decreased one order of magnitude after adding the reactions with HSA (Figure 4B).

Although we did not measure it, we simulated the nitrosation of the thiol in HSA by both radical ($^{\cdot}NO_2$) and N_2O_3 pathways (reactions 6-8 in Table II, Fig. 4C). In the absence of acceleration by protein, radical

Table II. Reactions used in the mathematical simulation

#	*Reaction*	*Rate constant*	*Ref.*
1	Stock → prolinonoate	0.31 s^{-1}	This work
2	prolinonoate → 2 ˙NO	0.077 s^{-1}	This work
3	2 ˙NO + O_2 → 2 $^{\cdot}NO_2$	2.8 × 10^6 $M^{-2}s^{-1}$	[5, 6, 8]
3 Ac	2 ˙NO + O_2 → 2 $^{\cdot}NO_2$	3.86 × 10^6 $M^{-2}s^{-1}$	This work
4	$^{\cdot}NO_2$ + ˙NO ←→ N_2O_3	1.1 × 10^9 $M^{-1}s^{-1}$ 8.1 × 10^4 s^{-1}	[5]
5	N_2O_3 → 2 HNO_2	9930 s^{-1}	[5, 15]
6	HSA + N_2O_3 → HSA-SNO + HNO_2	6.6 × 10^7 $M^{-1}s^{-1}$	[35]
7	HSA + $^{\cdot}NO_2$ → HSA-S˙ + HNO_2	2.2 × 10^7 $M^{-1}s^{-1}$	[36]
8	HSA-S˙ + ˙NO → HSA-SNO	3 × 10^9 $M^{-1}s^{-1}$	[37]
9	˙NO → NO_3^- (RBC)	498 s^{-1}	[38]

 https://doi.org/10.1016/j.niox.2019.01.014

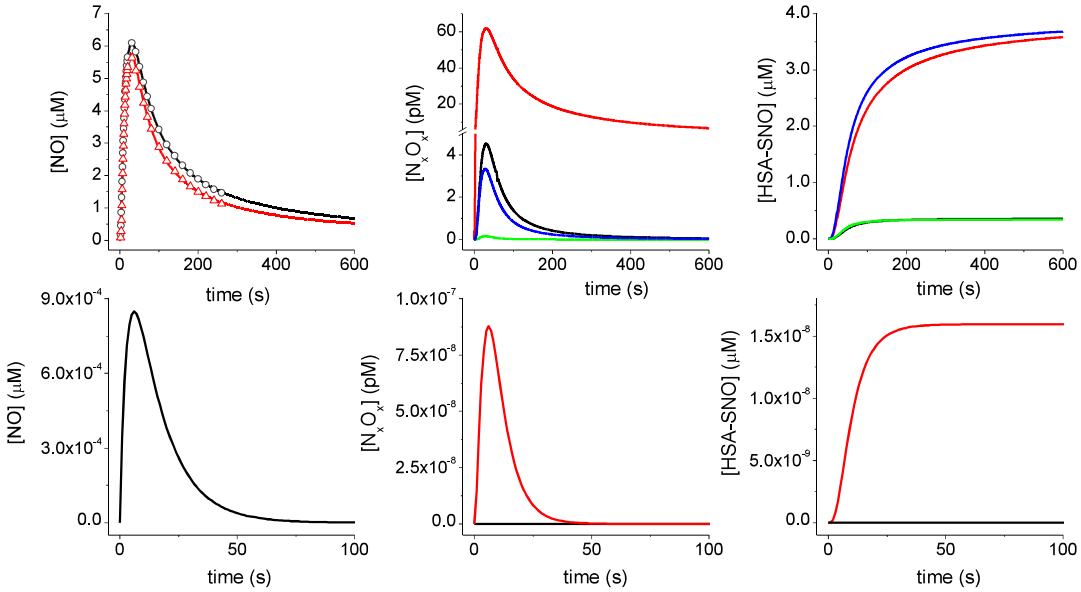

Figure 4. Mathematical modeling of ˙NO autoxidation. A) The experimental results for ˙NO autoxidation in buffer (black symbols) and in the presence of HSA (red symbols) in Figure 1A were correctly simulated by the mathematical model (lines). **B)** The transient concentrations of nitrogen dioxide (red) and dinitrogen trioxide (black) were determined to be in the pM range, and to decrease significantly by adding reactions with HSA (blue and green, for $^{\cdot}NO_2$ and N_2O_3 respectively). **C)** The theoretical nitrosation of HSA was found to occur mostly by the radical pathway (red, reactions 7-8 in Table II), vs N_2O_3 pathway (black, coincident with green, reaction 6 in Table II). Introducing the acceleration by HSA led to a higher rate of nitrosation, but overall similar yields in nitrosated products (blue and green for radical and N_2O_3-mediated nitrosation, respectively). **D)** To simulate the same experiment in whole blood, we introduced the reaction with red blood cells (reaction 9 in Table II) to the accelerated model and found that red blood cells consume virtually all of the ˙NO very rapidly. **E)** Red blood cells also cause a dramatic decrease in the formation of nitrogen oxides (references as in B). **F)** The effect of red blood cells on nitrosation is also dramatic and decreases HSA nitrosation 8 orders of magnitude (references as in C).

nitrosation yielded 10.3 times more nitrosothiol than N_2O_3-mediated nitrosation. After including acceleration by HSA, a slight increase in the rate of nitrosation was obtained, and the radical pathway yielded 10.6 times more nitrosated HSA than the N_2O_3 pathway, but the overall yield remains almost the same: 45 vs 46% relative to added ˙NO. Notice that the efficiency of nitrosation is high because we only considered this minimal model that is nonetheless useful to illustrate several points. For one, this accelerated nitrosation is expected to be of little consequence and difficult to assess experimentally, because there is only a small increase in the *rate (and not yield) of nitrosation*, that would be missed by experimental error.

Next we considered the whole blood scenario. In this case, ˙NO will react preferentially with oxyhemoglobin in red blood cells to form nitrate [39, 40]. To include this reaction in the simulation we had to consider the limitation imposed by the localization of hemoglobin inside red blood cells, that actually lowers the rate of ˙NO decomposition relative to free hemoglobin [38]. We used the rate constants determined by Liu *et al*. extrapolated to whole blood [38]. We still used prolinonoate as a short burst of ˙NO, that may be equated to a rapid and short release of ˙NO by cells. In this case, erythrocytes consume virtually all of the ˙NO that would be produced by

prolinonoate, lowering its concentration almost 4 orders of magnitude to sub-nanoMolar (Figure 4D). The concentration of the intermediates $^{\bullet}NO_2$ and N_2O_3 is lowered 8 orders of magnitude from picoMolar level (Figure 4E). The concentration of nitrosated HSA is also lowered 8 orders of magnitude from microMolar level (Figure 4F). Therefore, although the autoxidation of $^{\bullet}NO$ is accelerated by proteins, this effect will be of little consequence in $^{\bullet}NO$ physiology, especially in the vascular space. In the extravascular space, in the absence of red blood cells, the acceleration of $^{\bullet}NO$ autoxidation by proteins may contribute only a very small amount of nitrosating species, as suggested by the minor effect of protein acceleration on nitrosation in Figure 4C.

Discussion

This work fills a gap between the works of Nudler et al. and Keszler et al. regarding the interaction of $^{\bullet}NO$ with proteins [13-15]. The first publication suggested that the hydrophobic core of proteins could accumulate 120 times more $^{\bullet}NO$ than an equivalent volume of water, thus leading to micellar catalysis that was calculated to accelerate $^{\bullet}NO$ autoxidation 1.4×10^4 fold, which in turn translated into an enhanced nitrosation of protein and low molecular thiols [13]. This claim was later refuted by Keszler et al. who analyzed the system in depth by different approaches and found no increase in the nitrosation yields of either protein or low molecular weight thiols [15]. However, no study of the kinetics of $^{\bullet}NO$ disappearance in the presence of proteins was conducted in this work [15]. Yet, the idea that hydrophobic core of proteins could accelerate $^{\bullet}NO$ autoxidation sounded reasonable, so we performed experiments to specifically address this issue. Our results indicate that proteins can accelerate $^{\bullet}NO$ autoxidation but to a much lesser degree than first proposed.

Most of the volume of the proteins is occupied by the atoms of amino acids that present an atom density comparable to that of organic crystals. However, the packing of amino acids is not perfect and cavities are formed that are not directly accessible to the solvent neither occupied by any other atoms (see Figures S1-S4). Furthermore, proteins are not completely rigid structures and are known to undergo rapid structural fluctuations (the so called "protein breathing") [19]. As an example, it can be observed in Figure S1 how HSA can accommodate hydrophobic ligands such as myristic acid in previously inexistent cavities. Considering this protein dynamics, it could be envisioned that proteins could indeed favor the solubility of $^{\bullet}NO$ and O_2, increase their local concentration and accelerate the $^{\bullet}NO$ autoxidation reaction.

Our results show that HSA and other proteins are able to accelerate $^{\bullet}NO$ autoxidation in a manner that depends on the size and dynamics of the protein. HSA was the largest protein assessed, also the most dynamic protein according to measurements of compressibility, and the one that led to the largest acceleration of $^{\bullet}NO$ autoxidation. Structural alterations of HSA induced by decreasing pH include a partial unfolding, an increase in surface area and a decrease in protein compressibility [29, 30], and were found to decrease the acceleration of $^{\bullet}NO$ autoxidation (Figure 2). Besides HSA, other proteins were found to accelerate $^{\bullet}NO$ autoxidation in a size-dependent manner (Figure 3). These proteins also differed in their compressibility and a good correlation was found with the acceleration factor (Figure 3B), indicating an important role of the protein structural dynamics in facilitating $^{\bullet}NO$ and O_2 solubilization and reaction.

If we consider that this acceleration occurs by a similar mechanism to that in lipid membranes [6, 9, 41], then these results suggest that $^{\bullet}NO$ and O_2 are indeed more soluble in the hydrophobic core of proteins than in buffer. However, the measurement of O_2 solubility in horse plasma actually shows that proteins do not increase O_2 solubility relative to an isotonic solution [42]. This can be reconciled with our interpretation considering that O_2 is on average excluded from a large part of the volume occupied by the atoms of the protein but favorably located inside protein cavities that account approximately 2% of the total protein volume (Table 1). Taking into account the observed acceleration of $^{\bullet}NO$ autoxidation by proteins and its relationship with protein size, cavities and dynamics, it appears that the reaction is not accelerated by a single cavity, but that single steps may occur in different regions of the protein. In addition, we have to considered that $^{\bullet}NO$ autoxidation, even though is kinetically a termolecular reaction (Eq. 1 and 4), it actually involves two separate bimolecular steps and one homolysis [5, 43]:

$$^{\bullet}NO + O_2 \rightleftharpoons ONOO^{\bullet} \qquad \text{(Eq.7)}$$

$ONOO^{\bullet} + {}^{\bullet}NO \rightarrow ONOONO$ (Eq. 8)

$ONOONO \rightarrow 2\ {}^{\bullet}NO_2$ (Eq. 9)

Considering the high diffusivity of $^{\bullet}NO$ and O_2 [19, 44], it is likely that the acceleration of $^{\bullet}NO$ autoxidation by proteins can occur by the following mechanism. First, $^{\bullet}NO$ and O_2 locate transiently in different hydrophobic cavities within the protein (energetically more favorably than in water). While diffusing to another hydrophobic cavity, both $^{\bullet}NO$ and O_2 collide with each other in a channel that connects both cavities formed by the motion of the peptide chains, leading to the transient $ONOO^{\bullet}$. Next, a second molecule of $^{\bullet}NO$ that diffused to a nearby hydrophobic cavity reacts with $ONOO^{\bullet}$ and leads to ONOONO, that splits in two $^{\bullet}NO_2$ that diffuse to the aqueous phase. This theory explains why the acceleration of $^{\bullet}NO$ autoxidation depended greatly on protein dynamics (Figure 3B) and size, especially why there is a minimum size of protein that favors the acceleration (Figure 3C). Furthermore, it also explains why there is such an important decrease in A_C when HSA is partially unfolded at acid pH (Figure 2). Although the volume of HSA stays practically the same, there are fewer hydrophobic cavities where O_2 and $^{\bullet}NO$ can locate, and at the same time, these cavities are less connected to each other because of the higher rigidity of the protein.

To extrapolate our results to other biochemically relevant reactions such as nitrosation and to more biological scenarios such as the vascular space, we used mathematical simulations. With respect to nitrosation, the simulations were in agreement with results reported by Keszler et al. in that no significant increase in nitrosation yields was predicted, but only a minor increase in the rate of nitrosation, that would be very difficult to assess experimentally [15]. Although it has been discussed before, it is important to point out that the site of formation of nitrosating species will not necessarily favor the nitrosation of neighboring thiols, because the *rates* of nitrosation reactions (either radical or N_2O_3-mediated, reactions 6-8 in Table II) are not limited by diffusion [41]. This means that several collisions are needed before nitrosation occurs. Considering that diffusion is at least 100 times more rapid than reaction, it is more probable that the nitrosating species will diffuse and react far from the site of production. In this context, the presence of a highly reactive thiol may be more important for an efficient nitrosation rather than proximity to a source of nitrosating species. For instance, although $^{\bullet}NO$ autoxidation is accelerated in lipid membranes [6, 9], Zhang et al. showed that cysteine residues inserted at different depths in the membrane were less nitrosated than glutathione in the aqueous phase [45]. Although it may seem unexpected, this result is explained because it is the thiolate rather than the thiol that reacts rapidly with nitrosating species, and the ionization is energetically unfavorable in the low polarity milieu of the membrane [45].

In the vascular space, the simulations show that most of the $^{\bullet}NO$ will be rapidly consumed by red blood cells (Figure 4D) and that the acceleration by plasma HSA is not quantitatively significant as an alternative route to $^{\bullet}NO$ decomposition. In the extravascular space in the absence of red blood cells, the acceleration of $^{\bullet}NO$ autoxidation by HSA may theoretically be responsible for up to 27% of the products of autoxidation such as nitrite. However, plasma has other proteins that can react with $^{\bullet}NO$ through different mechanisms, such as ceruloplasmin, that has an important $^{\bullet}NO$ oxidase activity [46] and may effectively compete with HSA for $^{\bullet}NO$, narrowing even more the possible physiological effects of the acceleration of $^{\bullet}NO$ autoxidation by HSA.

Even though the relative importance of this protein-driven acceleration is not clear at present, the quantitative information provided here may be included in the future in more complex and realistic kinetic models of $^{\bullet}NO$ in the vasculature, and eventually understand its role in $^{\bullet}NO$ biology.

Acknowledgements

We are grateful to Dr Ernesto Cuevasanta and Dr Beatriz Alvarez for excellent suggestions and critical discussions.

Funding

This work was partially supported by grants C38-432 from Comisión Sectorial de Investigación Científica (CSIC) to AD, FCE_1_2017_1_136043 Fondo Clemente Estable from Agencia Nacional de Investigación e Innovación (ANII) to MNM. MNM and AD also acknowledge Sistema Nacional de

Investigadores (SNI) and Programa de Desarrollo de las Ciencias Básicas (PEDECIBA).

References

1. Moncada, S. and E. Higgs, *The discovery of nitric oxide and its role in vascular biology.* British journal of pharmacology, 2006. **147**(S1): p. S193-S201.
2. Hill, B.G., et al., *What part of NO don't you understand? Some answers to the cardinal questions in nitric oxide biology.* Journal of Biological Chemistry, 2010: p. jbc. R110. 101618.
3. Horst, B.G. and M.A. Marletta, *Physiological activation and deactivation of soluble guanylate cyclase.* Nitric Oxide, 2018. **77**: p. 65-74.
4. Ferrer-Sueta, G. and R. Radi, *Chemical biology of peroxynitrite: kinetics, diffusion, and radicals.* ACS chemical biology, 2009. **4**(3): p. 161-177.
5. Goldstein, S. and G. Czapski, *Kinetics of nitric oxide autoxidation in aqueous solution in the absence and presence of various reductants. The nature of the oxidizing intermediates.* Journal of the American Chemical Society, 1995. **117**(49): p. 12078-12084.
6. Möller, M.N., et al., *Membrane "lens" effect: focusing the formation of reactive nitrogen oxides from the NO/O_2 reaction.* Chem. Res. Toxicol., 2007. **20**: p. 709-714.
7. Ford, P.C., D.A. Wink, and D.M. Stanbury, *Autoxidation kinetics of aqueous nitric oxide.* Febs Letters, 1993. **326**(1-3): p. 1-3.
8. Kharitonov, V.G., A.R. Sundquist, and V.S. Sharma, *Kinetics of nitric oxide autoxidation in aqueous solution.* Journal of Biological Chemistry, 1994. **269**(8): p. 5881-5883.
9. Liu, X., et al., *Accelerated reaction of nitric oxide with O2 within the hydrophobic interior of biological membranes.* Proceedings of the National Academy of Sciences, 1998. **95**(5): p. 2175-2179.
10. Möller, M.N., et al., *Solubility and diffusion of oxygen in phospholipid membranes.* Biochimica et Biophysica Acta (BBA)-Biomembranes, 2016. **1858**(11): p. 2923-2930.
11. Marrink, S., R. Sok, and H. Berendsen, *Free volume properties of a simulated lipid membrane.* The Journal of chemical physics, 1996. **104**(22): p. 9090-9099.
12. Shiva, S., et al., *Nitric oxide partitioning into mitochondrial membranes and the control of respiration at cytochrome c oxidase.* Proceedings of the National Academy of Sciences, 2001. **98**(13): p. 7212-7217.
13. Rafikova, O., R. Rafikov, and E. Nudler, *Catalysis of S-nitrosothiols formation by serum albumin: the mechanism and implication in vascular control.* Proc. Natl. Acad. Sci. U.S.A., 2002. **99**(9): p. 5913-5918.
14. Nedospasov, A., et al., *An autocatalytic mechanism of protein nitrosylation.* Proceedings of the national academy of sciences, 2000. **97**(25): p. 13543-13548.
15. Keszler, A., Y. Zhang, and N. Hogg, *Reaction between nitric oxide, glutathione, and oxygen in the presence and absence of protein: How are S-nitrosothiols formed?* Free Radical Biology and Medicine, 2010. **48**(1): p. 55-64.
16. Liang, J. and K.A. Dill, *Are proteins well-packed?* Biophysical journal, 2001. **81**(2): p. 751-766.
17. Prange, T., et al., *Exploring hydrophobic sites in proteins with xenon or krypton.* Proteins: Structure, Function, and Bioinformatics, 1998. **30**(1): p. 61-73.
18. Curry, S., et al., *Crystal structure of human serum albumin complexed with fatty acid reveals an asymmetric distribution of binding sites.* Nature Structural Biology, 1998. **5**: p. 827.
19. Lakowicz, J.R. and G. Weber, *Quenching of protein fluorescence by oxygen. Detection of structural fluctuations in proteins on the nanosecond time scale.* Biochemistry, 1973. **12**(21): p. 4171-4179.
20. Möller, M. and A. Denicola, *Study of protein-ligand binding by fluorescence.* Biochemistry and Molecular Biology Education, 2002. **30**(5): p. 309-312.
21. Möller, M., et al., *Direct measurement of nitric oxide and oxygen partitioning into liposomes and low density lipoprotein.* J. Biol. Chem., 2005. **280**(10): p. 8850-4.
22. Voss, N.R. and M. Gerstein, *3V: cavity, channel and cleft volume calculator and extractor.* Nucleic acids research, 2010. **38**(suppl_2): p. W555-W562.
23. Bhattacharya, A.A., S. Curry, and N.P. Franks, *Binding of the general anesthetics propofol and halothane to human serum albumin. High resolution crystal structures.* J Biol Chem, 2000. **275**(49): p. 38731-8.
24. Transue, T.R., et al., *X-ray and NMR characterization of covalent complexes of trypsin, borate, and alcohols.* Biochemistry, 2004. **43**(10): p. 2829-39.
25. Stein, P.E., et al., *Crystal structure of uncleaved ovalbumin at 1.95 A resolution.* J Mol Biol, 1991. **221**(3): p. 941-59.
26. Harata, K., *X-ray structure of a monoclinic form of hen egg-white lysozyme crystallized at 313 K. Comparison of two independent molecules.* Acta Crystallogr D Biol Crystallogr, 1994. **50**(Pt 3): p. 250-7.
27. Pettersen, E.F., et al., *UCSF Chimera--a visualization system for exploratory research and analysis.* J Comput Chem, 2004. **25**(13): p. 1605-12.
28. Hoops, S., et al., *COPASI—a complex pathway simulator.* Bioinformatics, 2006. **22**(24): p. 3067-3074.
29. Peters, T.J., *2. The albumin molecule: its structure and chemical properties*, in *All about albumin: biochemistry, genetics and medical applications*, T.J. Peters, Editor. 1996, Academic Press: San Diego, California. p. 9-78.

30. El Kadi, N., et al., *Unfolding and refolding of bovine serum albumin at acid pH: ultrasound and structural studies.* Biophys. J., 2006. **91**: p. 3397-3404.
31. Baler, K., et al., *Electrostatic unfolding and interactions of albumin driven by pH changes: a molecular dynamics study.* The Journal of Physical Chemistry B, 2014. **118**(4): p. 921-930.
32. Gekko, K., *Volume and Compressibility of Proteins*, in *High Pressure Bioscience: Basic Concepts, Applications and Frontiers*, K. Akasaka and H. Matsuki, Editors. 2015, Springer Netherlands: Dordrecht. p. 75-108.
33. Gekko, K. and Y. Hasegawa, *Compressibility-structure relationship of globular proteins.* Biochemistry, 1986. **25**: p. 6563-6571.
34. Gekko, K. and H. Noguchi, *Compressibility of globular proteins in water at 25C.* J. Phys. Chem., 1979. **83**(21): p. 2706-2714.
35. Keshive, M., et al., *Kinetics of S-Nitrosation of Thiols in Nitric Oxide Solutions.* Chemical Research in Toxicology, 1996. **9**(6): p. 988-993.
36. Ford, E., M.N. Hughes, and P. Wardman, *Kinetics of the reactions of nitrogen dioxide with glutathione, cysteine, and uric acid at physiological pH.* Free Radical Biology and Medicine, 2002. **32**(12): p. 1314-1323.
37. Madej, E., et al., *Thiyl radicals react with nitric oxide to form S-nitrosothiols with rate constants near the diffusion-controlled limit.* Free Radic Biol Med, 2008. **44**(12): p. 2013-8.
38. Liu, X., et al., *Diffusion-limited reaction of free nitric oxide with erythrocytes.* Journal of biological chemistry, 1998. **273**(30): p. 18709-18713.
39. Herold, S., M. Exner, and T. Nauser, *Kinetic and Mechanistic Studies of the NO•-Mediated Oxidation of Oxymyoglobin and Oxyhemoglobin.* Biochemistry, 2001. **40**(11): p. 3385-3395.
40. Joshi, M.S., et al., *Nitric oxide is consumed, rather than conserved, by reaction with oxyhemoglobin under physiological conditions.* Proceedings of the National Academy of Sciences, 2002. **99**(16): p. 10341-10346.
41. Moller, M.N., et al., *Acceleration of nitric oxide autoxidation and nitrosation by membranes.* IUBMB Life, 2007. **59**(4-5): p. 243-8.
42. Sendroy, J., R.T. Dillon, and D.D. Van Slyke, *Studies of gas and electrolyte equilibria in blood XIX. The solubility and physical state of uncombined oxygen in blood.* Journal of Biological Chemistry, 1934. **105**(3): p. 597-632.
43. Kissner, R., *Reaction Steps in Nitrogen Monoxide Autoxidation*, in *Advances in Inorganic Chemistry*. 2015, Elsevier. p. 335-354.
44. Möller, M.N. and A. Denicola, *Diffusion of nitric oxide and oxygen in lipoproteins and membranes studied by pyrene fluorescence quenching.* Free Radical Biology and Medicine, 2018. **128**: p. 137-143.
45. Zhang, H., et al., *Decreased S-nitrosation of peptide thiols in the membrane interior.* Free Radical Biology and Medicine, 2009. **47**(7): p. 962-968.
46. Shiva, S., et al., *Ceruloplasmin is a NO oxidase and nitrite synthase that determines endocrine NO homeostasis.* Nature chemical biology, 2006. **2**(9): p. 486.